ACS APPLIED MATERIALS & INTERFACES

www.acsami.org

Research Article

Femtosecond Laser-Induced Supermetalphobicity for Design and Fabrication of Flexible Tactile Electronic Skin Sensor

Chengjun Zhang, Zhikang Li, Haoyu Li, Qing Yang,* Hao Wang, Chao Shan, Jingzhou Zhang, Xun Hou, and Feng Chen*

Cite This: *ACS Appl. Mater. Interfaces* 2022, 14, 38328−38338

Read Online

ACCESS | Metrics & More | Article Recommendations | Supporting Information

ABSTRACT: Pursuing flexible tactile electronic skin sensors with superior comprehensive performances is highly desired in practical applications. However, current flexible tactile electronic skin sensors suffer insufficient flexibility and sensitivity, as well as high-cost and low-efficiency in fabrication, and are susceptible to contamination in sensing performances. Here, a highly sensitive all-flexible tactile sensor (AFTS) is presented with capacitive sensing that combines a double-side micropyramids dielectric layer and a liquid metal (LM) electrode. The design and fabrication of LM-based AFTS are based on supermetalphobicity induced by femtosecond laser. The supermetalphobic micropyramids lead to a high sensitivity up to 2.78 kPa^{-1}, an ultralow limit of detection of ∼3 Pa, a fast response time of 80 ms, and an excellent durability of cyclic load over 10 000 times. The used femtosecond laser enables programmable, high-efficiency, low-cost, and large-scale fabrication of supermetalphobic double-side micropyramids, which is difficult to implement using conventional techniques. Furthermore, the outer substrates are treated by a femtosecond laser, endowing the AFTS with excellent antifouling performance and stable sensing signals in the highly humid environment. Successful monitoring of human physiological and motion signals demonstrates the potential of our developed AFTS for wearable biomonitoring applications.

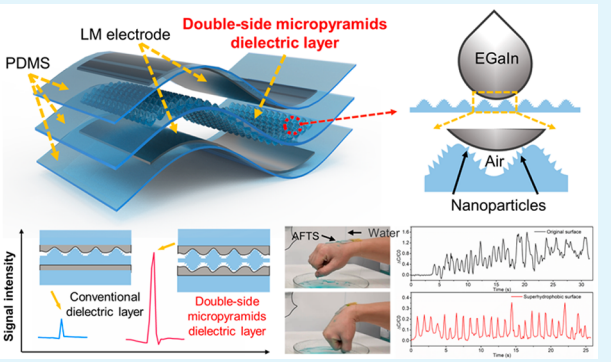

KEYWORDS: *flexible tactile electronic skin sensors, double-side micropyrmaids, liquid metal, supermetalphobicity, femtosecond laser fabrication*

1. INTRODUCTION

Flexible tactile electronic skin sensors have human-skin-mimicking flexibility and functions, which can be conformally attached to human skin or robotics surface to perceive various stimuli such as pressure, stress, temperature, and so on, showing promising applications in fields of personalized healthcare, human machine interface, and intelligent robotics.[1−3] In practical application, pressure perception is of great significance because of its ability to detect various physical motions and biosignals, such as gentle touch, wrist pulse, heartbeat, and respiration rate.[4−7] In the past decade, a large number of flexible wearable pressure sensors have been developed, and most of them are based on piezoresistive,[4,8] capacitive,[7,9,10] piezoelectric,[11,12] and triboelectric properties.[13] Among all these sensing principles, capacitive pressure sensors, which are composed of a dielectric elastomeric layer sandwiched between two electrodes and transduce pressure changes into capacitance variation, have been intensively investigated because of their simple structures, low power consumption, and temperature-insensitive features. In pursuit of capacitive pressure sensors with desirable sensing performance and structure robustness, both dielectric elastomeric layers and electrodes are crucial.

The materials that are used for the electrodes are significant, and they affect the flexibility, stretchability, and stability of capacitive pressure sensors. Currently, indium tin oxide (ITO) conducting polymer, poly(3,4-ethylenedioxythiophene): poly(styrenesulfonate) (PEDOT:PSS),[14−16] and nanomaterial-polymer composite such as Ag nanowires,[17,18] carbon nanotubes (CNTs),[19,20] graphene,[21] and so on, have been widely employed as flexible electrodes for capacitive pressure sensors. However, these materials generally feature a Young's modulus that is orders of magnitude larger than that of human skin (∼10 kPa),[15] degrading the devices flexibility and conformability when worn on human bodies. In recent years, a rapidly developing flexible conductive material, gallium-based liquid metal (LM), has attracted researcher's interests worldwide. Because of its excellent electrical/thermal conductivity,[5,22−24] intrinsically

Received: May 18, 2022
Accepted: July 31, 2022
Published: August 11, 2022

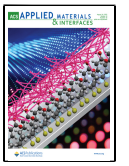

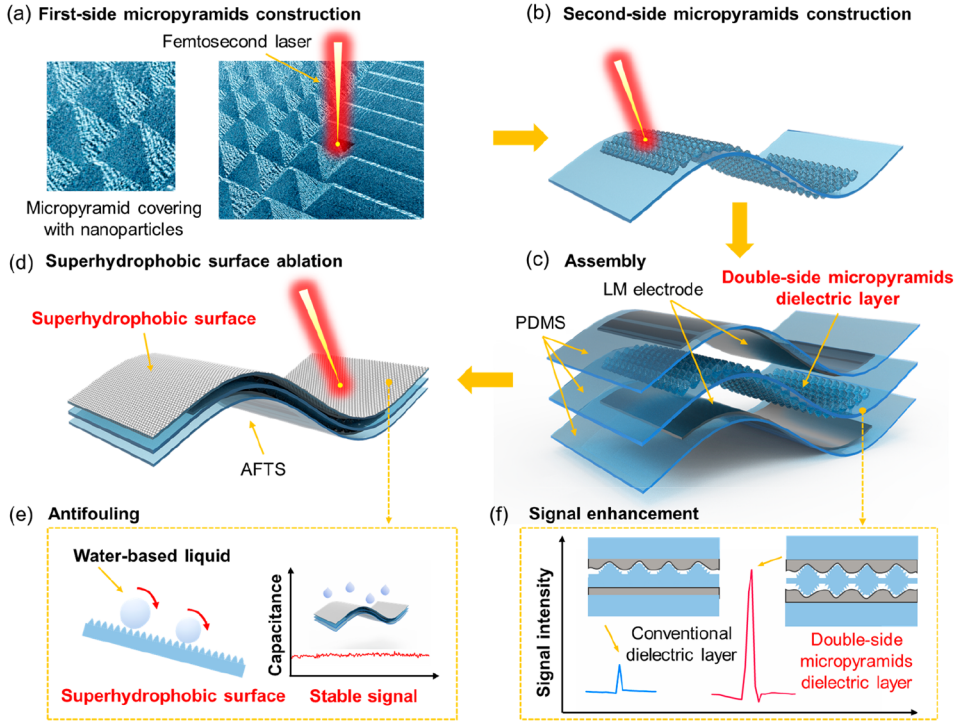

Figure 1. Design and principle of the AFTS. (a) Construction of micropyramid on PDMS by a femtosecond laser. (b) Construction of double-side micropyramids dielectric layer. (c) Assembly of the capacitive pressure sensor. (d) Superhydrophobic surface prepared by a femtosecond laser ablation. (e) Performance of antifouling of capacitive pressure sensor. (f) Principle of enhancement of signal intensity.

superb stretchability,[25] biocompatibility, and zero-closed Young's modulus,[7,26−30] LM is widely considered as an ideal alternative for constructuring extremely conductive and soft flexible electrodes, and have been used in wearable devices,[5,31−33] soft robotics,[34] flexible actuators,[35] and so on. However, owing to the amorphic liquid phase of LM, achieving a highly sensitive, and robust flexible pressure sensor remains a big challenge.[33,36−43] Therefore, a new strategy has to be invented to obtain a highly sensitive LM-based capacitive sensor, enabling their practical applications in biomonitoring which requires high sensitivity.

To improve the sensing performance of capacitive pressure sensors, microstructured elastomeric dielectric layers have been proved to be an effective strategy, which can increase the compressibility and decrease the viscosity, thus improving the sensitivity, limit of detection (LOD), and response time.[14] Using this strategy, a diversity of microstructured dielectric layers have been constructed in the past decade, including micropyramids,[14,44] microdomes,[45,46] micropillars,[47,48] and so on.[1,49] Significant improvement has been achieved in pressure sensitivity and response speed. Therefore, it is possible to improve the sensitivity of the LM-based pressure sensor by manufacturing the elastomeric dielectric layer with microstructures. However, LM is easily oxidized in the air to form a highly adhesive oxide layer on its surface, which can adhere to most surfaces.[50−53] The adherence between the dielectric layer and the LM electrode is the main reason why the conventional microstructuring method is not appropriate for enhancing the sensitivity of the LM-based sensors. Therefore, stability and durability or structure robustness of LM electrode-based wearable sensors are still unsolved challenges, hindering their practical applications.

Herein, we successfully demonstrated a highly sensitive all-flexible tactile sensor (AFTS) using LM as the electrodes and supermetalphobic double-side polydimethylsiloxane (PDMS) micropyramid arrays as the dielectric layer with a femtosecond laser fabrication technique. Compared with conventional one-side micropyramid structures, the proposed double-side micropyramids dielectric layer can contribute to a significant improvement in pressure sensitivity, LOD, and response time because of its enhanced compressibility and reduced viscosity. The femtosecond laser technique has two remarkable advantages: (1) realizing programmable, high-efficiency, low-cost, large-scale fabrication of a double-side micropyramid; (2) endowing a micropyramid with a supermetalphobic surface by manufacturing a nanoparticle-based surface structure, which can prevent dilaceration of LM from substrates and thus improves the durability of the LM electrodes. Additionally, the surfaces of the PDMS-based outer substrate is further treated superhydrophobically by the femtosecond laser technique, bringing the AFTS a skin-surpassing function (i.e., antifouling capacity). The antifouling capacity can resolve the base capacitance shift caused by water-based contaminants, significantly improving the performance stability during the long-term use of the capacitive tactile sensor. The assembled tactile sensor shows a high sensitivity (2.78 kPa^{-1}), low LOD (~3 Pa), excellent durability (>10000 times cyclic loads), and fast response time (80 ms). It also shows great sensing ability under various complex deformations due to the use of all-flexible materials. Furthermore, it can maintain stable sensing signals in the highly humid environment and maintains repellence to water after 1000 cycles of 100% stretching. Successful monitoring of various human physical motions and physiological signals, such as finger bending, foot pressure, pulse wave, and so on, demonstrate the great potential of our developed AFTS in applications of

https://doi.org/10.1021/acsami.2c08835
ACS Appl. Mater. Interfaces 2022, 14, 38328−38338

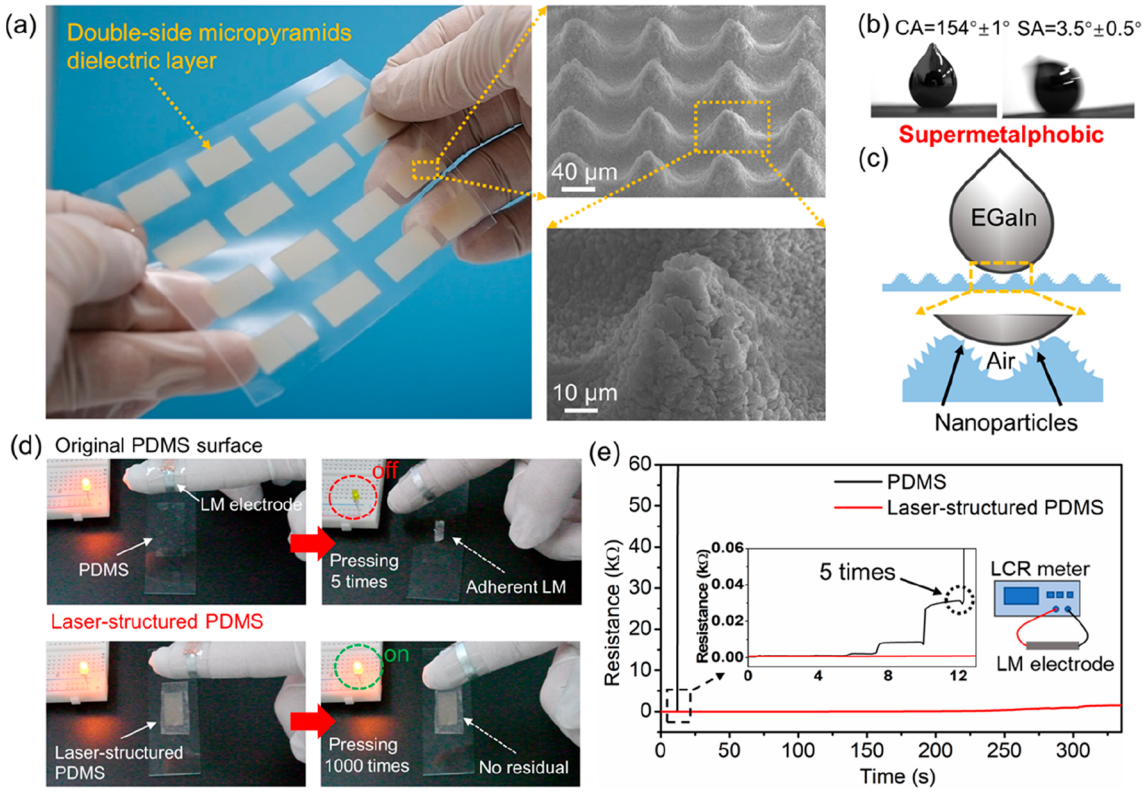

Figure 2. Femtosecond laser-structured dielectric layer for robust LM-based capacitance sensor. (a) Photo of a large-scale laser-structured dielectric layer arrays and SEM image of the micropyramid arrays. (b,c) Wettability and schematic of the LM on the laser-structured dielectric layer. (d) Photo of the process of pressing the LM electrode on the original PDMS and laser-structured PDMS. (e) Resistance change of the LM electrode during the repeated pressing process on the PDMS and laser-structured PDMS.

wearable biomonitoring, human-machine interfaces, and soft robotic systems.

2. RESULTS AND DISCUSSION

2.1. Construction of Double-Side Micropyramid-Based Capacitive Pressure Sensors. The structure schematic of our proposed capacitive pressure sensors is shown in Figure 1, in which the supermetalphobic double-side PDMS micropyramids are used as the dielectric layer, the LM as the electrodes, and the outer PDMS with superhydrophobic surfaces as the substrates of the entire device. The fabrication process of our proposed capacitive pressure sensors starts with femtosecond laser ablating a flat PDMS line-by-line to produce microgrooves and then orthogonally crossed ablating to form micropyramids with nanoparticles covering their surfaces (Figure 1a, Figure S1, Supporting Information). Sequentially, the one-side microstructured PDMS is turned over and ablated to produce micropyramids by a femtosecond laser in a similar way, resulting in a double-side micropyramids layer, which features supermetalphobicity because of the abundant nanoparticles (Figure 1b). Then, the PDMS printed with LM electrodes and double-side micropyramids dielectric layer are assembled by means of lamination under a certain pressure (Figure 1c). Finally, the outer surfaces of the assembled sensor are scanned by a femtosecond laser, finishing the fabrication of the capacitive pressure sensors (Figure 1d, Figure S2, Supporting Information).

The femtosecond laser-based fabrication technique features following several advantages: (1) realizing the programmable, high-efficiency, low-cost, and large-scale fabrication of double-side micropyramid dielectric layers that achieve significant improvement in sensing performance compared with the previously reported LM-based pressure sensor (Figure 1f, Table S1, Supporting Information);[33,36−43] (2) inducing abundant nanoparticles on the surface of the micropyramid to repel the LM; and (3) endowing the AFTS with antifouling capability by constructing a superhydrophobic surface, significantly improving the long-term stability in a high-humidity environment (Figure 1e).

Enabled by the high-precision processing and superior controllability, the femtosecond laser technique can offer a promising route for facile and streamlined fabrication of supermetalphobic double-side micropyramids dielectric layer. Figure 2a displays the 4 × 4 arrays of double-side micropyramids dielectric layer fabricated on the PDMS substrate. The micropyramids can be fabricated on a PDMS films with arbitrary thickness in one step by the femtosecond laser technique, and it is very easy to construct a double-side micropyramids dielectric layer. Moreover, abundant nanoparticles are induced during the preparation of the micropyramid (Figure S3, Supporting Information).

The stability of LM electrodes is crucial for capacitive sensors. LM easily adheres to most of the surface owing to its high-adhesion oxygen layer. When the LM is used as a flexible electrode, nonstick surface of the dielectric layer is necessary to ensure the stability of the sensor in the process of repeated pressing. Our femtosecond laser microstructuring technique overcomes the adhesion issue between the LM and dielectric layer.[54,55] The LM droplet shows a high adhesion on the original PDMS surface with a contact angle (CA) of 146 ± 2° and a

https://doi.org/10.1021/acsami.2c08835
ACS Appl. Mater. Interfaces 2022, 14, 38328−38338

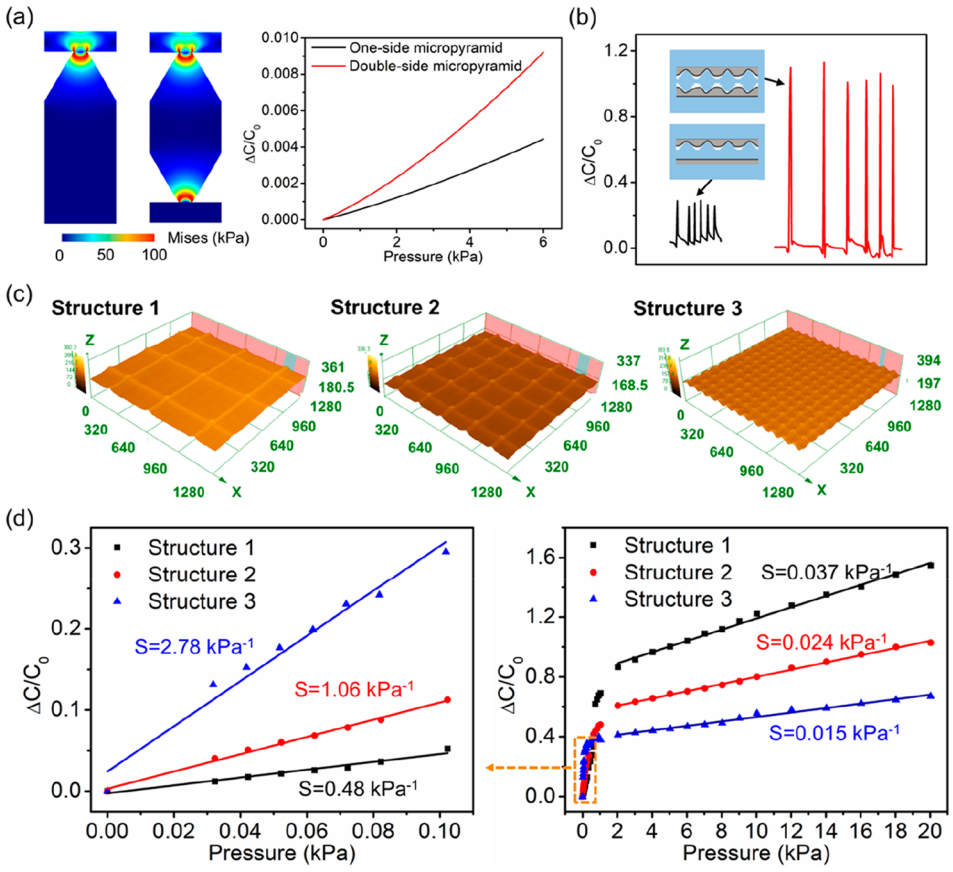

Figure 3. Tunable sensitivity of AFTS with double-side micropyramid dielectric layer. (a) Stress distribution and capacitance changes of COMSOL simulation results for conventional dielectric layer and double-side micropyramid dielectric layer under 6 kPa pressure. (b) Signal intensity of capacitance when an external pressure applied on the sensor with one-side micropyramids and double-side micropyramids dielectric layer, respectively. (c) 3D morphology of the different arrangements of double-side micropyramids. (d) Sensor sensitivity curves with three different types of dielectric layers.

sliding angle (SA) > 90° (Figure S4, Supporting Information). In contrast, the larger CA of 154 ± 1° and the SA of 3.5 ± 0.5° of the LM are measured on the dielectric layer with a micropyramid (Figure 2b, Figure S4, Supporting Information). This nonstick dielectric layer is defined as supermetalphobic surface. The nonstick dielectric layer is attributed to the existence of abundant nanoparticles, which leads to the significant reduction of the contact area between the LM and the surface of the micropyramid (Figure 2c).

We further investigate whether the laser-structured dielectric layer can maintain supermetalphobicity under external pressure. We use a LM electrode to press on a smooth PDMS and a laser-structured PDMS respectively to observe whether the LM electrode would be damaged. A light emitting diode (LED) is connected to LM electrode to observe the electrical conductivity (Figure S5, Supporting Information). When pressing on the smooth PDMS dielectric layer, the LM electrode adheres to the surface of PDMS (Figure 2d). After five times pressing on the smooth surface of PDMS, the LM electrode is completely damaged (Figure S6, Supporting Information). The LED light lamp is extinguished, and the resistance of the LM electrode increases sharply (Figure 2e). In contrast, the LM electrode will not stick to the laser-structured dielectric layer. Even after 1000 times pressing on a laser-structured PDMS, the LM electrode can maintain excellent electrical conductivity (Figure 2d, e, Figure S7, Supporting Information). The above results show that the dielectric layer with supermetalphobic micropyramid can realize the high robustness of the LM-based capacitive sensor. These results indicate that the femtosecond laser-based fabrication technique could potentially serve as an ideal alternative to templet, etching, and photolithography with a higher degree of flexibility in the choice of designs based on applicational demands.

2.2. Performance Enhancement and Tunability Evaluation of Femtosecond Laser Fabricated Double-Side Micropyramids. To elucidate the underlying mechanism of the double-side micropyramids dielectric layer enabled sensitivity enhancement, we compare the conventional one-side micropyramids and double-side micropyramids dielectric layer by COMSOL simulation (Figure 3a). Constructing micropyramid structures on PDMS film provides more space to replace the compressed materials under external pressure, therefore improving the compressibility of the PDMS dielectric layer. Thus, microstructuring the PDMS film is an effective way to reduce the viscosity and elastic resistance. Double-side microstructures prepared by a femtosecond laser provide more spaces to further minimize the problems associated with viscoelastic behavior. Therefore, it results in better sensing properties as a dielectric layer compared with the conventional one-side microstructures. When LM is used as a flexible electrode, the output signals of a capacitive pressure sensor with double-side micropyramids arrays are remarkably improved compared with the sensor with a conventional one-side micropyramids dielectric layer (Figure 3b). This can be attributed to three

https://doi.org/10.1021/acsami.2c08835
ACS Appl. Mater. Interfaces 2022, 14, 38328−38338

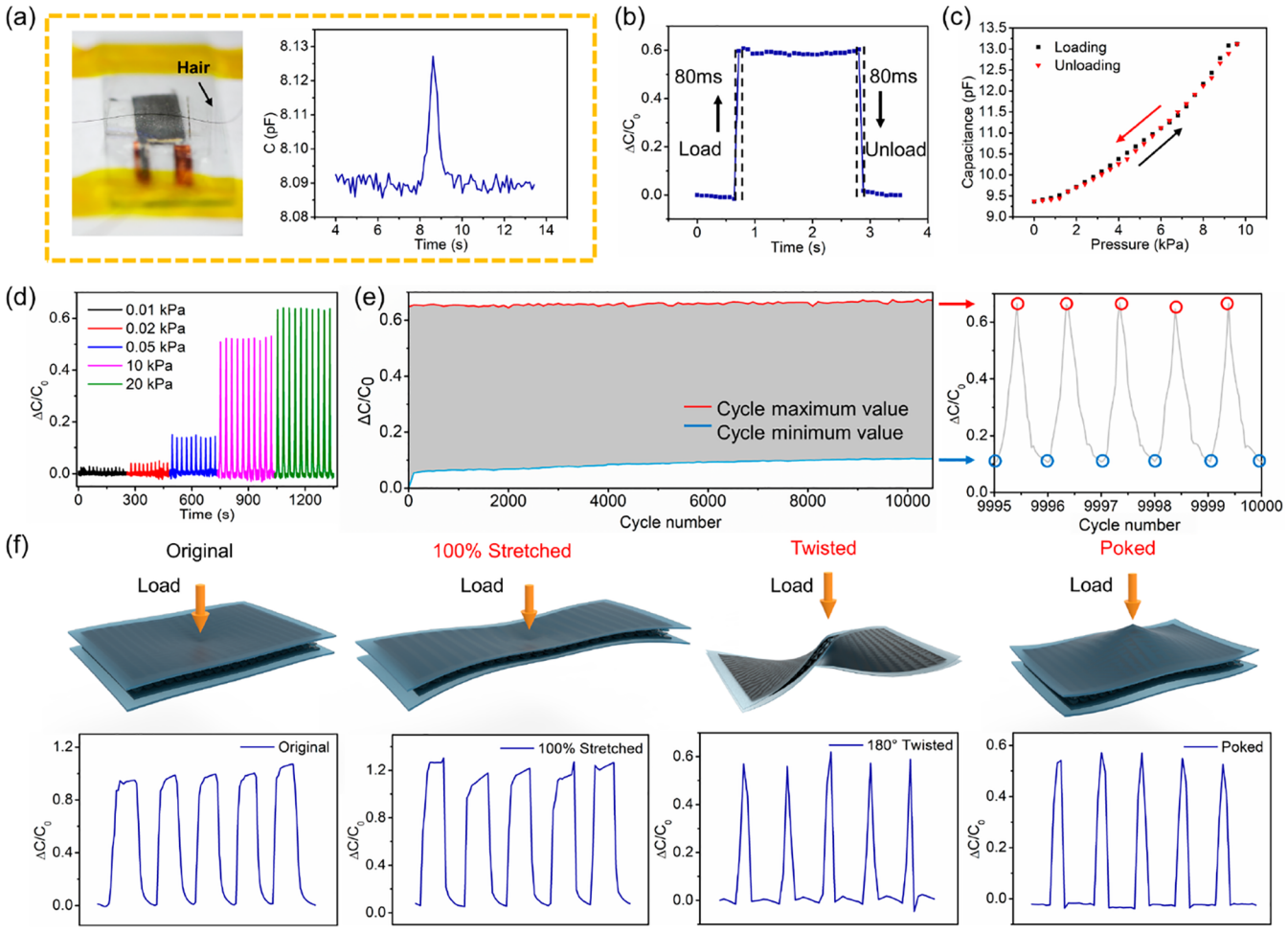

Figure 4. Characterizations of AFTS. (a) Capacitance change of sensor under a hair pressing (the corresponding pressure: ~3 Pa). (b) Instant response time of sensor. (c) Capacitance change of sensor during the loading and unloading process. (d) Normalized capacitance changes under different cyclic pressures. (e) Cycling stability at a pressure of 20 kPa for 10 000 cycles. (f) Normalized capacitance changes of sensor under various deformations of 100% stretching, twisting, and poking.

main factors: (1) there is lower elastic resistance to external pressure in the double-side micropyramids dielectric layer because of more air voids in the PDMS film; (2) since the elastic modulus of LM is much lower than that of the PDMS layer, the surface area of adjacent electrodes will change when the LM electrodes make contact with the micropyramids of the dielectric layer; and (3) when the double-side micropyramids dielectric layer is compressed, both the air (dielectric constant ε = 1.0) between the two sides of the dielectric layer can be displaced by PDMS ($\varepsilon \sim 3.0$).

Having explored the mechanism of the double-side micropyramids dielectric layer-based pressure sensors, we further investigated its performance tunability by changing the micropyramid size and arrangements (Figure 3c, Figure S7, Supporting Information). The pressure performance test is carried out between 0 and 20 kPa, which covered the pressure range of all mechanical signals of the human body. The sensitivity of the sensor can be controlled by tuning the arrangement of the micropyramid arrays. The maximum sensitivity among these three sensors in the low-pressure region (from 0−0.1 kPa) is 2.78 kPa^{-1} (Structure 3), but the sensitivity decreased to the minimum value of 0.015 kPa^{-1} when the pressure increased above 1 kPa. Conversely, the pressure sensitivity of the sensor with structure 1 is the lowest (0.48 kPa^{-1}) in the low-pressure region but the highest (0.037 kPa^{-1}) in the high-pressure region (Figure 3d). The reason for this phenomenon can be explained as below: in the low-pressure region (below 0.1 kPa), the $\Delta C/C_0$ is mainly due to the permittivity change between the two adjacent electrode when external pressure is applied on the surface of the sensor, that is, the contribution to the $\Delta C/C_0$ of the $\Delta\varepsilon$ is greater than that of the Δd; when the pressure increases gradually, the sensor with structure 1 is more likely to lead to larger Δd than that of thr sensor with structure 3, which is attributable to a reduced deformability of the dielectric layer under high pressure. Therefore, the contribution of Δd to $\Delta C/C_0$ is greater than that of the $\Delta\varepsilon$ in the high-pressure region. In practical application, the pressure sensitivity can be tuned by different arrangements and sizes of the micropyramid, so that the measured pressure is always within the optimal performance range of the sensor.

Figure 4 shows the performance of our femtosecond laser fabricated pressure sensor with a supermetalphobic double-side dielectric layer. The LOD of the sensor is an important parameter, which determines whether weak signals could be perceived. The sensor can detect the placement or removal of an ultrasmall weight such as a hair pressing, which corresponds to a pressure of ~3 Pa (Figure 4a). The sensor also shows a fast

https://doi.org/10.1021/acsami.2c08835
ACS Appl. Mater. Interfaces 2022, 14, 38328−38338

response time of 80 ms in the loading and unloading process, with a pressure of 20 kPa (Figure 4b). The hysteresis error of the sensor is only 4.12% (Figure 4c). A slight increase in hysteresis after more than 1000 cycling testing is possibly due to the fatigue damage of the PDMS (Figure S8, Supporting Information). To characterize the stability of the sensor, we test the $\Delta C/C_0$ under different pressure cycles (Figure 4d) and the capacitance of the sensor under long-time loading process (Figure S9, Supporting Information). The sensor exhibits distinguishable responses under various cyclic pressure of 0.01, 0.02, 0.05, 10, and 20 kPa. The durability of the sensor under the long-term cyclic loading is a crucial factor which influences the robust application of the tactile sensor. As shown in Figure 4e and S10 (Supporting Information), the capacitive response of the tactile sensor also remains unchanged after 10 000 compression/release cycles under the pressure of 20 kPa, demonstrating ultrahigh durability of the AFTS.

The AFTS is inevitably deformed in the practical application, so it is of great importance to maintain good pressure perception performances under various complex deformations. As shown in Figure 4f and Figure S11 (Supporting Information), the sensing ability of AFTSs is well maintained under the deformation of 100% stretching, 180° twisting, and poking, respectively. When the sensor is stretched at 100%, the range of $\Delta C/C_0$ is almost the same as that of the original state, indicating that large strain deformation has negligible effect on the pressure detection capability of the AFTS. Even though the sensor is subjected to the deformation of 180° torsion or poking, it still has the ability to perceive external pressure. These excellent performances demonstrated the application potential of the AFTS in the field of human wearable electronics. Our fabricated AFTS shows extraordinarily high performance superior to that of other reported LM-based tactile sensors in the literature (Figure 5, Table S1).[33,36−43]

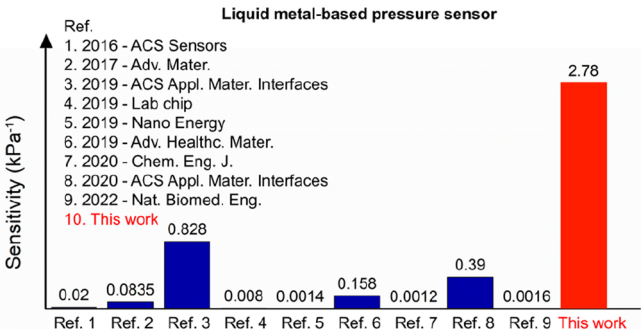

Figure 5. Comparison of the sensitivity of the previously reported LM-based pressure sensor.

2.3. Antifouling Performance of Superhydrophobic AFTS. When the capacitive pressure sensor is applied as wearable electronics, the sensing performance will be inevitably affected by the water-based contaminant sticking to the surface of the sensor. We fabricate a superhydrophobic surface by a femtosecond laser ablation to endow the capacitive pressure sensor with the capacity of antifouling performance. As shown in the SEM images of Figure 6a, the original surface of PDMS is very smooth. Dropping a 5 μL water droplet on the original surface of the PDMS substrate, the contact angle (CA) of the water droplet is 112.4° ± 1.2°. Moreover, the water droplet will adhere tightly to the original surface of the PDMS even when placing the sample vertically. On the contrary, the surface ablated by the femtosecond laser has abundant nanoparticles (Figure 6b). The CA of the water droplet on the superhydrophobic surface is 153.2° ± 1.5°. The water droplet will roll and slide from the sample surface with a small angle of inclination (SA = 3.6° ± 1.6°). The contact area between the water droplets and the surface of the PDMS is largely reduced by micro/nanostructures constructed by femtosecond laser; thus, the adhesive force is almost negligible between the water and PDMS surface. According to the Cassie wetting model, the contact angle between water and PDMS surface is greater than 150°, so it is superhydrophobic. The surface ablated by femtosecond laser endows the capacitive pressure sensor with an antifouling property for common water-based contaminants (Figure 6c, Figure S12, Supporting Information) and the ability of stable sensing under a high humid environment (Figure 6d−f). When dropping water gradually on the original surface of the sensor, the water droplets gradually accumulate into large droplets and stick on the surface of the sensor, resulting in the increase of the capacitance of sensor (Figure 6d). Conversely, the droplets roll away from the superhydrophobic surface directly, and the capacitance of the sensor fluctuated slightly around the initial value without increasing. In addition, when dripping water gradually on the surface of sensor, the sensor with a superhydrophobic surface can output stable signals without a base capacitance shift when applying a cycle pressure on the sensor and testing the wrist joint movements (Figure 6e,f, Movie S1, Supporting Information).

To verify the durability of the superhydrophobicity of the femtosecond laser-ablated PDMS surface, we test the wettability of water droplet under 1000 cycles of 100% stretching of PDMS substrate. As shown in Figure 6g, the CA of water droplet on this surface is always >150°, and the SA is <10°, indicating that the femtosecond laser-ablated surface maintains excellent superhydrophobicity under cyclic large elastic deformation. For the superhydrophobic surface, a water droplet on the surface is at the Cassie wetting state[56−60] and is repelled by the superhydrophobicity of the nanoparticles of the PDMS substrate. The nanoparticles are directly induced on the surface of the PDMS substrate by a femtosecond laser and will not fall off during the cyclic elastic deformations (Figure S13, Supporting Information). Therefore, the Cassie wetting state of water on the femtosecond laser ablated surface would not be destroyed under large elastic deformation. At the same time, the sensor can maintain a stable pressure detection performance after 1000 cycles of 50% tensile deformation (Figure S14, Supporting Information). The antifouling sensor fabricated by a femtosecond laser can significantly improve the stability of sensing signals of capacitive pressure sensor in high-humidity environment and shows high durability of superhydrophobicity, which are very important for wearable electronics in practical applications.

2.4. Applications of AFTS in Human Motion Monitoring. To demonstrate the application potential of the prepared AFTS in wearable biomonitoring, the sensors are attached to different parts of the human body for biomonitoring. As depicted in Figure 7a, the sensor is attached to the wrist to monitor the human pulse signal in real time, and the characteristic peaks of the pulse could be clearly distinguished from pulse waves. Similarly, when the sensor is attached to different positions of the wrist, it can detect the movement of the palm (Figure 7b). To further test the signal detection performance of the sensor under different deformation conditions, the sensors are attached to different joints (finger,

https://doi.org/10.1021/acsami.2c08835
ACS Appl. Mater. Interfaces 2022, 14, 38328−38338

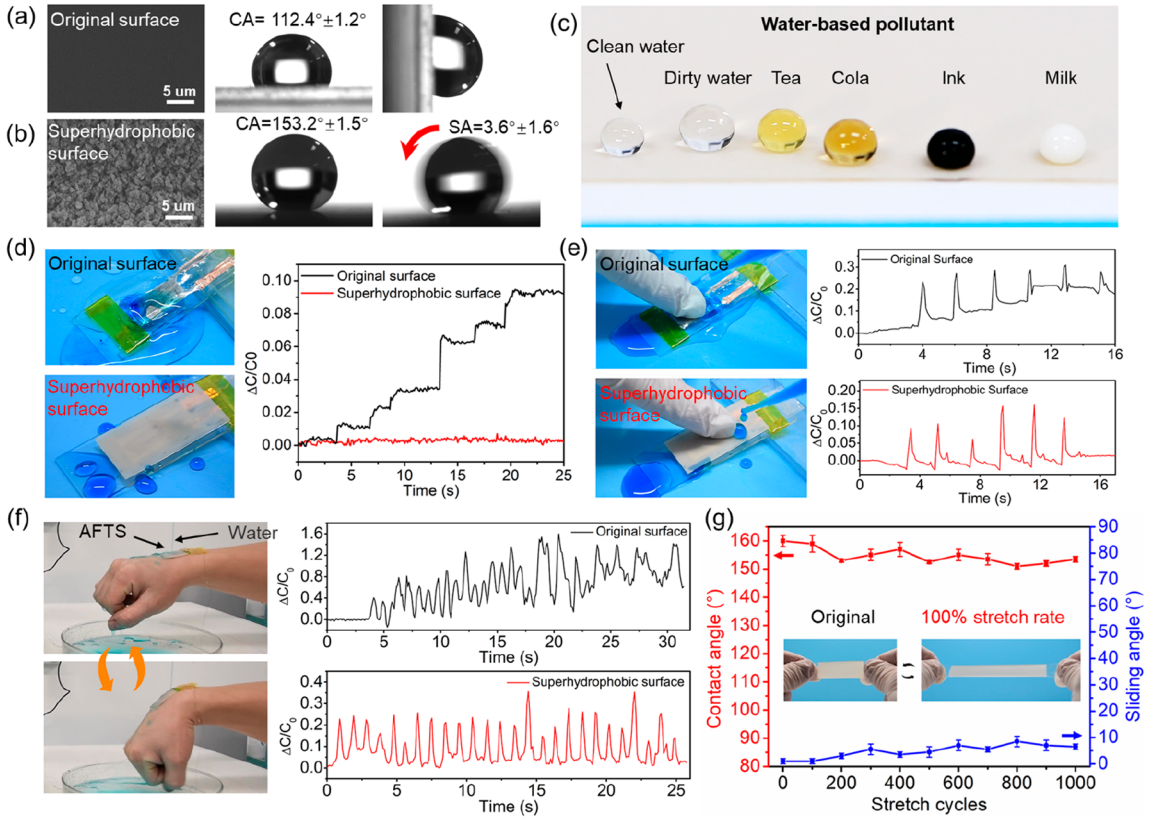

Figure 6. Antifouling features of the AFTS. (a,b) SEM images and wettability of the water on the surface of original and superhydrophobic surface of PDMS respectively. (c) Photo of the droplet of water-based pollutant on the superhydrophobic surface of PDMS. (d,e) Capacitance curve of the sensor with original and superhydrophobic surface during the process of dropping water gradually and pressing at the same time. (f) Capacitance curve of the sensor attached on the wrist when pouring the water on the sensor. (g) Durability of superhydrophobic property of PDMS surface during 1000 cycles of 100% stretching.

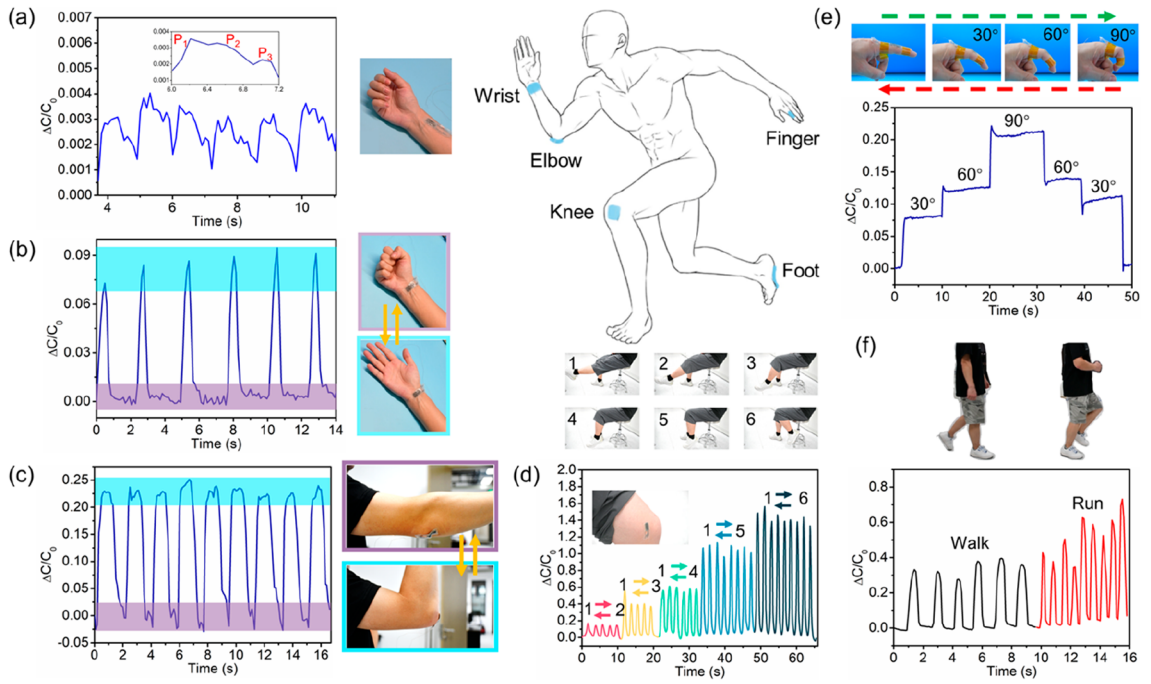

Figure 7. Wearable AFTS for mechanical signal monitors. Real-time monitoring of (a) human wrist pulse and (b) palm movement. $\Delta C/C_0$ of the sensor in response to (c) elbow bending, (d) knee bending, (e) finger bending, and (f) walking and running movement.

https://doi.org/10.1021/acsami.2c08835
ACS Appl. Mater. Interfaces 2022, 14, 38328−38338

elbow, knee, etc.) or foot for the detection of human mechanical signals. Figure 7c shows the $\Delta C/C_0$ of the sensor in response to the bending of the elbow. When the elbow is bent from 0° to 90°, the changes in the normalized capacitance of the sensor change accordingly. Similarly, when the sensor is attached to the knee, the sensor could clearly sense the different bending amplitude of the knee joint, and the electrical signals are highly repeatable and stable (Figure 7d). When the sensor is attached at the finger joint, the changes in the normalized capacitance increase accordingly when the finger is sequentially bent for 0°, 30°, 60°, and 90°. The normalized capacitance of the sensor could fully recover to the initial value when the finger is straightened gradually (Figure 7e). The above results show that the sensor can rapidly response to joint motion (bending angle changes), and the signal values have good stability. When the sensor is attached to the foot of the volunteer, the movements of walking and running could be distinguished by the amplitude and frequency of the output signal (Figure 7f). In summary, the experimental results show that the sensor can effectively monitor various mechanical signals (from weak to strong signals) of the human body as wearable devices and can distinguish mechanical signals in different states (strong or weak, high or low frequency), demonstrating promising application potential in the field of human−machine interaction and human health monitoring.

3. CONCLUSION

We demonstrate a highly sensitive AFTS with capacitive sensing utilizing double-side micropyramids as dielectric layer and LM/PDMS as electrode/substrate. The femtosecond laser fabricated double-side micropyramids dielectric layer significantly improves the pressure sensitivity, LOD, and response time because of its enhanced compressibility and reduced viscosity in comparison with conventional one-side micropyramids. The supermetalphobic micropyramids enable an ultrahigh durability of the LM electrode due to the abundant nanoparticles induced by a femtosecond laser. The proposed femtosecond laser can realize programmable, high-efficiency, low-cost, and large-scale fabrication of double-side micropyramids in a simple manner, which is difficult to implement using conventional techniques, such as templet, etching, and lithography. Furthermore, the outer substrates are superhydrophobically treated by the femtosecond laser and endow the AFTS with excellent antifouling ability and stable sensing signals in the highly humid environment. Additionally, the superhydrophobic surface shows ultrahigh durability and can maintain its repellence to water over 1000 cycles of 100% stretching. The resultant AFTS shows a pressure sensitivity of 2.78 kPa^{-1}, ultralow pressure detection limit of ∼3 Pa, fast response time of 80 ms, and ultrahigh cycle durability more than 10 000 times. The AFTS can perceive the external pressure under complex deformations because of the preparation by all-flexible materials. The successful use of the AFTS for monitoring of various human physiological and motion signals demonstrates its potential for applications of wearable biomonitoring, human−machine interfaces, and soft robotic systems.

4. EXPERIMENTAL SECTION

4.1. Materials. The LM used in our experiment is EGaIn (Wochang Metal Co., Ltd.), which has a melting point of 12 °C. PDMS layers are finished thin films purchased from Hangzhou Bald Advanced Materials Co., Ltd.

4.2. Preparation of the AFTS. *4.2.1. Fabrication of the Microstructures.* As an extreme manufacturing method, the femtosecond laser has been used to construct microstructures on the surface of various materials for the preparation of functional surfaces.[61−65] Here, we structure the micropyramids of dielectric layer (150 μm in thickness) by a femtosecond laser orthogonally crossed line-by-line ablation, and nanoparticles of surface of capacitive pressure sensor by a femtosecond laser typical line-by-line scanning (Figure S15, Supporting Information). As shown in Figure S16 (Supporting Information), a femtosecond laser beam (with a pulse duration of 50 fs, central wavelength of 800 nm and repetition frequency of 1 kHz) from a Ti:sapphire laser system (Coherent, Librausp 1K-he200) is vertically focused onto the surface of the PDMS sheet by a plano-convex lens (focal length of 200 mm) in air. The PDMS substrate is fixed on a computer-controlled moveable platform. The laser power is held constant at 300 mW and the moving speed of the platform is 50 μm/s. Adjusting the adjacent distance (AD) of laser scanning can realize the structures with different functions we need. The interval of the adjacent distance (AD) of laser scanning lines is set at 100 μm for fabrication of the micropyramid arrays of the dielectric layer and 50 μm for fabrication of nanoparticles on the surface of a capacitive pressure sensor, respectively (Figure S17, Supporting Information).

4.2.2. Patterning the LM Electrode. As shown in Figure S18 (Supporting Information), the PDMS support layers of LM electrode are 50 μm thick. First, the mask plate of the designed pattern is covered on the PDMS surface, and then the LM is poured onto the surface of PDMS substrate covering with the mask. Finally, the mask plate is slowly removed to form a patterned LM electrode on the surface of PDMS (Figure S19, Supporting Information).

4.2.3. Assembly of the AFTS. The sensors are assembled by bonding the dielectric layer and PDMS supporting layer printed with LM electrode after oxygen plasma treatment (Figure S18, Supporting Information). First, the copper electrode is stuck to the LM electrode of the PDMS support layer for subsequent testing, and then this surface is bonded to the one side of the dielectric layer to form a stable electrode connection and encapsulation. Then, the copper electrode is connected to the LM electrode by repeating the previous step, and the support layer with LM is bonded to the other side of the dielectric layer to form the final sensor. The prepared ultraflexible tactile sensor can withstand complex elastic deformation, such as stretching, twisting, and squeezing (Figure S20, Supporting Information).

4.3. Characterization. The surface microstructures of the samples are observed by a Flex 1000 scanning electron microscope (SEM; Hitachi, Japan). The wettability of liquid EGaIn droplet and water droplet on the sample surface is investigated by a JC2000D contact angle (CA) system (Powereach, China). The three-dimensional (3D) morphology of the surface of the micropyramid arrays is characterized through a LEXT-OLS4000 laser confocal microscope (Olympus, Japan). The capacitance is measured by a WK4100 LCR meter (Wayne Kerr Electronics, U.K.). All capacitance signals are tested at a frequency of 1 MHz. The volunteers for the motion detection measurements shown in Figures 6 and 7 are C. Z. and H. L., who gave their informed, written consent to wear the device.

■ ASSOCIATED CONTENT

Supporting Information

The Supporting Information is available free of charge at https://pubs.acs.org/doi/10.1021/acsami.2c08835.

Experimental details, femtosecond laser fabricating method, process of assembly of the AFTS, extra characterization results, comparison of performance of the liquid metal-based flexible tactile sensor (PDF)

Stable sensing performance of the antifouling liquid metal sensor in a highly humid environment (MP4)

https://doi.org/10.1021/acsami.2c08835
ACS Appl. Mater. Interfaces 2022, 14, 38328−38338

AUTHOR INFORMATION

Corresponding Authors

Feng Chen − *State Key Laboratory for Manufacturing System Engineering and Shaanxi Key Laboratory of Photonics Technology for Information, School of Electronic Science and Engineering, Xi'an Jiaotong University, Xi'an 710049, People's Republic of China*; orcid.org/0000-0002-7031-7404; Email: chenfeng@mail.xjtu.edu.cn

Qing Yang − *School of Mechanical Engineering, Xi'an Jiaotong University, Xi'an 710049, People's Republic of China*; Email: yangqing@mail.xjtu.edu.cn

Authors

Chengjun Zhang − *School of Mechanical Engineering, Xi'an Jiaotong University, Xi'an 710049, People's Republic of China*

Zhikang Li − *School of Mechanical Engineering, Xi'an Jiaotong University, Xi'an 710049, People's Republic of China*

Haoyu Li − *State Key Laboratory for Manufacturing System Engineering and Shaanxi Key Laboratory of Photonics Technology for Information, School of Electronic Science and Engineering, Xi'an Jiaotong University, Xi'an 710049, People's Republic of China*

Hao Wang − *School of Mechanical Engineering, Xi'an Jiaotong University, Xi'an 710049, People's Republic of China*

Chao Shan − *State Key Laboratory for Manufacturing System Engineering and Shaanxi Key Laboratory of Photonics Technology for Information, School of Electronic Science and Engineering, Xi'an Jiaotong University, Xi'an 710049, People's Republic of China*

Jingzhou Zhang − *State Key Laboratory for Manufacturing System Engineering and Shaanxi Key Laboratory of Photonics Technology for Information, School of Electronic Science and Engineering, Xi'an Jiaotong University, Xi'an 710049, People's Republic of China*

Xun Hou − *State Key Laboratory for Manufacturing System Engineering and Shaanxi Key Laboratory of Photonics Technology for Information, School of Electronic Science and Engineering, Xi'an Jiaotong University, Xi'an 710049, People's Republic of China*

Complete contact information is available at: https://pubs.acs.org/10.1021/acsami.2c08835

Author Contributions

C.Z.: Conceptualization, methodology, visualization, data curation, writing-original draft. H.L.: Methodology, validation, Z.L.: visualization, writing-review, and editing. Q.Y.: Resources, supervision, conceptualization, supervision, writing-review, and editing. H.W.: Data curation. C.S.: Methodology. J.Z.: Methodology. X.H.: Supervision. F.C.: Resources, supervision, conceptualization, supervision, writing-review, and editing.

Notes

The authors declare no competing financial interest.

ACKNOWLEDGMENTS

This work is supported by the National Science Foundation of China under the Grant Nos. 61875158, 62175195, and 12127806; the International Joint Research Laboratory for Micro/Nano Manufacturing and Measurement Technologies, and the Fundamental Research Funds for the Central Universities.

REFERENCES

(1) Chang, Y.; Wang, L.; Li, R.; Zhang, Z.; Wang, Q.; Yang, J.; Guo, C. F.; Pan, T. First Decade of Interfacial Iontronic Sensing: From Droplet Sensors to Artificial Skins. *Adv. Mater.* **2021**, *33*, 2003464.

(2) Gao, Y.; Yu, L.; Yeo, J. C.; Lim, C. T. Flexible Hybrid Sensors for Health Monitoring: Materials and Mechanisms to Render Wearability. *Adv. Mater.* **2020**, *32*, 1902133.

(3) Pyo, S.; Lee, J.; Bae, K.; Sim, S.; Kim, J. Recent Progress in Flexible Tactile Sensors for Human-Interactive Systems: From Sensors to Advanced Applications. *Adv. Mater.* **2021**, *33*, 2005902.

(4) Araromi, O. A.; Graule, M. A.; Dorsey, K. L.; Castellanos, S.; Foster, J. R.; Hsu, W. H.; Passy, A. E.; Vlassak, J. J.; Weaver, J. C.; Walsh, C. J.; Wood, R. J. Ultra-Sensitive and Resilient Compliant Strain Gauges for Soft Machines. *Nature* **2020**, *587*, 219.

(5) Ma, Z.; Huang, Q.; Xu, Q.; Zhuang, Q.; Zhao, X.; Yang, Y.; Qiu, H.; Yang, Z.; Wang, C.; Chai, Y.; Zheng, Z. Permeable Superelastic Liquid-Metal Fibre Mat Enables Biocompatible and Monolithic Stretchable Electronics. *Nat. Mater.* **2021**, *20*, 859.

(6) Chun, S.; Kim, J.-S.; Yoo, Y.; Choi, Y.; Jung, S. J.; Jang, D.; Lee, G.; Song, K.-I.; Nam, K. S.; Youn, I.; Son, D.; Pang, C.; Jeong, Y.; Jung, H.; Kim, Y.-J.; Choi, B.-D.; Kim, J.; Kim, S.-P.; Park, W.; Park, S. An Artificial Neural Tactile Sensing System. *Nat. Electron.* **2021**, *4*, 429.

(7) Lee, J.; Ihle, S. J.; Pellegrino, G. S.; Kim, H.; Yea, J.; Jeon, C.-Y.; Son, H.-C.; Jin, C.; Eberli, D.; Schmid, F.; Zambrano, B. L.; Renz, A. F.; Forró, C.; Choi, H.; Jang, K.-I.; Küng, R.; Vörös, J. Stretchable and Suturable Fibre Sensors for Wireless Monitoring of Connective Tissue Strain. *Nat. Electron.* **2021**, *4*, 291.

(8) Leber, A.; Dong, C.; Chandran, R.; Das Gupta, T.; Bartolomei, N.; Sorin, F. Soft and Stretchable Liquid Metal Transmission Lines as Distributed Probes of Multimodal Deformations. *Nat. Electron.* **2020**, *3*, 316.

(9) Sun, J. Y.; Keplinger, C.; Whitesides, G. M.; Suo, Z. Ionic Skin. *Adv. Mater.* **2014**, *26*, 7608.

(10) Wang, S.; Xu, J.; Wang, W.; Wang, G. N.; Rastak, R.; Molina-Lopez, F.; Chung, J. W.; Niu, S.; Feig, V. R.; Lopez, J.; Lei, T.; Kwon, S. K.; Kim, Y.; Foudeh, A. M.; Ehrlich, A.; Gasperini, A.; Yun, Y.; Murmann, B.; Tok, J. B.; Bao, Z. Skin Electronics from Scalable Fabrication of an Intrinsically Stretchable Transistor Array. *Nature* **2018**, *555*, 83.

(11) Chen, S.; Xin, S.; Yang, L.; Guo, Y.; Zhang, W.; Sun, K. Multi-Sized Planar Capacitive Pressure Sensor with Ultra-High Sensitivity. *Nano energy* **2021**, *87*, 106178.

(12) Wang, Z. L.; Song, J. Piezoelectric Nanogenerators Based on Zinc Oxide Nanowire Arrays. *Science* **2006**, *312*, 242.

(13) Shi, Y.; Wang, F.; Tian, J.; Li, S.; Fu, E.; Nie, J.; Lei, R.; Ding, Y.; Chen, X.; Wang, Z. L. Self-Powered Electro-Tactile System for Virtual Tactile Experiences. *Sci. Adv.* **2021**, *7*, eabe2943.

(14) Mannsfeld, S. C.; Tee, B. C.; Stoltenberg, R. M.; Chen, C. V.; Barman, S.; Muir, B. V.; Sokolov, A. N.; Reese, C.; Bao, Z. Highly Sensitive Flexible Pressure Sensors with Microstructured Rubber Dielectric Layers. *Nat. Mater.* **2010**, *9*, 859.

(15) Matsuhisa, N.; Chen, X.; Bao, Z.; Someya, T. Materials and Structural Designs of Stretchable Conductors. *Chem. Soc. Rev.* **2019**, *48*, 2946.

(16) Zhao, P.; Zhang, R.; Tong, Y.; Zhao, X.; Zhang, T.; Tang, Q.; Liu, Y. Strain-Discriminable Pressure/Proximity Sensing of Transparent Stretchable Electronic Skin Based on PEDOT:PSS/SWCNT Electrodes. *ACS Appl. Mater. Interfaces* **2020**, *12*, 55083.

(17) Xu, F.; Zhu, Y. Highly Conductive and Stretchable Silver Nanowire Conductors. *Adv. Mater.* **2012**, *24*, 5117.

(18) Guan, F.; Xie, Y.; Wu, H.; Meng, Y.; Shi, Y.; Gao, M.; Zhang, Z.; Chen, S.; Chen, Y.; Wang, H.; Pei, Q. Silver Nanowire−Bacterial Cellulose Composite Fiber-Based Sensor for Highly Sensitive Detection of Pressure and Proximity. *ACS Nano* **2020**, *14*, 15428.

(19) Lipomi, D. J.; Vosgueritchian, M.; Tee, B. C.; Hellstrom, S. L.; Lee, J. A.; Fox, C. H.; Bao, Z. Skin-Like Pressure and Strain Sensors Based on Transparent Elastic Films of Carbon Nanotubes. *Nat. Nanotechnol.* **2011**, *6*, 788.

(20) Kim, S. Y.; Park, S.; Park, H. W.; Park, D. H.; Jeong, Y.; Kim, D. H. Highly Sensitive and Multimodal All-Carbon Skin Sensors Capable of Simultaneously Detecting Tactile and Biological Stimuli. *Adv. Mater.* **2015**, *27*, 4178.
(21) Chen, S.; Wang, Y.; Yang, L.; Karouta, F.; Sun, K. Electron-Induced Perpendicular Graphene Sheets Embedded Porous Carbon Film for Flexible Touch Sensors. *Nano-Micro. Lett.* **2020**, *12*, 136.
(22) Zavabeti, A.; Ou, J. Z.; Carey, B. J.; Syed, N.; Orrell-Trigg, R.; Mayes, E. L. H.; Xu, C.; Kavehei, O.; O'Mullane, A. P.; Kaner, R. B.; Kalantar-Zadeh, K.; Daeneke, T. A Liquid Metal Reaction Environment for the Room-Temperature Synthesis of Atomically Thin Metal Oxides. *Science* **2017**, *358*, 332.
(23) Veerapandian, S.; Jang, W.; Seol, J. B.; Wang, H.; Kong, M.; Thiyagarajan, K.; Kwak, J.; Park, G.; Lee, G.; Suh, W.; You, I.; Kilic, M. E.; Giri, A.; Beccai, L.; Soon, A.; Jeong, U. Hydrogen-Doped Viscoplastic Liquid Metal Microparticles for Stretchable Printed Metal Lines. *Nat. Mater.* **2021**, *20*, 533.
(24) Yun, G.; Tang, S. Y.; Sun, S.; Yuan, D.; Zhao, Q.; Deng, L.; Yan, S.; Du, H.; Dickey, M. D.; Li, W. Liquid Metal-Filled Magneto-rheological Elastomer with Positive Piezoconductivity. *Nat. Commun.* **2019**, *10*, 1300.
(25) Wagner, S.; Bauer, S. Materials for Stretchable Electronics. *MRS Bull.* **2012**, *37*, 207.
(26) Dickey, M. D. Stretchable and Soft Electronics using Liquid Metals. *Adv. Mater.* **2017**, *29*, 1606425.
(27) Ottaviano, L.; Filipponi, A.; Di Cicco, A. Supercooling of Liqdui-Metal Droplets for X-Ray-Absorption-Spectroscopy Investigations. *Phys. Rev. B Condens Matter.* **1994**, *49*, 11749.
(28) Larsen, R. J.; Dickey, M. D.; Whitesides, G. M.; Weitz, D. A. Viscoelastic Properties of Oxide-Coated Liquid Metals. *J. Rheol.* **2009**, *53*, 1305.
(29) Liu, T.; Sen, P.; Kim, C.-J. Characterization of Nontoxic Liquid-Metal Alloy Galinstan for Applications in Microdevices. *J. Micro-electromech. Syst.* **2012**, *21*, 443.
(30) Kim, J. H.; Kim, S.; So, J. H.; Kim, K.; Koo, H. J. Cytotoxicity of Gallium−Indium Liquid Metal in an Aqueous Environment. *ACS Appl. Mater. Interfaces* **2018**, *10*, 17448.
(31) Gu, L.; Poddar, S.; Lin, Y.; Long, Z.; Zhang, D.; Zhang, Q.; Shu, L.; Qiu, X.; Kam, M.; Javey, A.; Fan, Z. A Biomimetic Eye with a Hemispherical Perovskite Nanowire Array Retina. *Nature* **2020**, *581*, 278.
(32) Xu, K.; Fujita, Y.; Lu, Y.; Honda, S.; Shiomi, M.; Arie, T.; Akita, S.; Takei, K. A Wearable Body Condition Sensor System with Wireless Feedback Alarm Functions. *Adv. Mater.* **2021**, *33*, 2008701.
(33) Zhang, C.; Liu, S.; Huang, X.; Guo, W.; Li, Y.; Wu, H. A Stretchable Dual-Mode Sensor Array for Multifunctional Robotic Electronic Skin. *Nano energy* **2019**, *62*, 164.
(34) Wang, H.; Chen, S.; Yuan, B.; Liu, J.; Sun, X. Liquid Metal Transformable Machines. *Acc. Mater. Res.* **2021**, *2*, 1227.
(35) Wu, J.; Tang, S. Y.; Fang, T.; Li, W.; Li, X.; Zhang, S. A Wheeled Robot Driven by a Liquid-Metal Droplet. *Adv. Mater.* **2018**, *30*, 1805039.
(36) Liao, M.; Liao, H.; Ye, J.; Wan, P.; Zhang, L. Polyvinyl Alcohol-Stabilized Liquid Metal Hydrogel for Wearable Transient Epidermal Sensors. *ACS Appl. Mater. Interfaces* **2019**, *11*, 47358.
(37) Zhang, Y.; Liu, S.; Miao, Y.; Yang, H.; Chen, X.; Xiao, X.; Jiang, Z.; Chen, X.; Nie, B.; Liu, J. Highly Stretchable and Sensitive Pressure Sensor Array Based on Icicle-Shaped Liquid Metal Film Electrodes. *ACS Appl. Mater. Interfaces* **2020**, *12*, 27961.
(38) Yeo, J. C.; Kenry; Yu, J.; Loh, K. P.; Wang, Z.; Lim, C. T. Triple-State Liquid-Based Microfluidic Tactile Sensor with High Flexibility, Durability, and Sensitivity. *ACS Sensors* **2016**, *1*, 543.
(39) Kim, K.; Choi, J.; Jeong, Y.; Cho, I.; Kim, M.; Kim, S.; Oh, Y.; Park, I. Highly Sensitive and Wearable Liquid Metal-Based Pressure Sensor for Health Monitoring Applications: Integration of a 3D-Printed Microbump Array with the Microchannel. *Adv. Healthc. Mater.* **2019**, *8*, 1900978.
(40) Gao, Y.; Ota, H.; Schaler, E. W.; Chen, K.; Zhao, A.; Gao, W.; Fahad, H. M.; Leng, Y.; Zheng, A.; Xiong, F.; Zhang, C.; Tai, L. C.; Zhao, P.; Fearing, R. S.; Javey, A. Wearable Microfluidic Diaphragm Pressure Sensor for Health and Tactile Touch Monitoring. *Adv. Mater.* **2017**, *29*, 1701985.
(41) Lou, Y.; Liu, H.; Zhang, J. Liquid Metals in Plastics for Super-Toughness and High-Performance Force Sensors. *Chem. Eng. J.* **2020**, *399*, 125732.
(42) Zhou, X.; Zhang, R.; Li, L.; Zhang, L.; Liu, B.; Deng, Z.; Wang, L.; Gui, L. A Liquid Metal Based Capacitive Soft Pressure Microsenso. *Lab Chip* **2019**, *19*, 807.
(43) Nan, K.; Babaee, S.; Chan, W. W.; Kuosmanen, J. L. P.; Feig, V. R.; Luo, Y.; Srinivasan, S. S.; Patterson, C. M.; Jebran, A. M.; Traverso, G. Low-Cost Gastrointestinal Manometry via Silicone−Liquid-Metal Pressure Transducers Resembling a Quipu. *Nat. Biomed. Eng.* **2022**, DOI: 10.1038/s41551-022-00859-5.
(44) Li, Z.; Zhang, S.; Chen, Y.; Ling, H.; Zhao, L.; Luo, G.; Wang, X.; Hartel, M. C.; Liu, H.; Xue, Y.; Haghniaz, R.; Lee, K.; Sun, W.; Kim, H.; Lee, J.; Zhao, Y.; Zhao, Y.; Emaminejad, S.; Ahadian, S.; Ashammakhi, N.; Dokmeci, M. R.; Jiang, Z.; Khademhosseini, A. Gelatin Methacryloyl-Based Tactile Sensors for Medical Wearables. *Adv. Funct. Mater.* **2020**, *30*, 2003601.
(45) Lee, Y.; Park, J.; Cho, S.; Shin, Y. E.; Lee, H.; Kim, J.; Myoung, J.; Cho, S.; Kang, S.; Baig, C.; Ko, H. Flexible Ferroelectric Sensors with Ultrahigh Pressure Sensitivity and Linear Response over Exceptionally Broad Pressure Range. *ACS Nano* **2018**, *12*, 4045.
(46) Bae, G. Y.; Pak, S. W.; Kim, D.; Lee, G.; Kim, D. H.; Chung, Y.; Cho, K. Linearly and Highly Pressure-Sensitive Electronic Skin Based on a Bioinspired Hierarchical Structural Array. *Adv. Mater.* **2016**, *28*, 5300.
(47) Qiu, Z.; Wan, Y.; Zhou, W.; Yang, J.; Yang, J.; Huang, J.; Zhang, J.; Liu, Q.; Huang, S.; Bai, N.; Wu, Z.; Hong, W.; Wang, H.; Guo, C. F. Ionic Skin with Biomimetic Dielectric Layer Templated from Calathea Zebrine Leaf. *Adv. Funct. Mater.* **2018**, *28*, 1802343.
(48) Su, Q.; Huang, X.; Lan, K.; Xue, T.; Gao, W.; Zou, Q. Highly Sensitive Ionic Pressure Sensor Based on Concave Meniscus for Electronic Skin. *J. Micromech. Microeng.* **2020**, *30*, 015009.
(49) Zheng, Y.; Lin, T.; Zhao, N.; Huang, C.; Chen, W.; Xue, G.; Wang, Y.; Teng, C.; Wang, X.; Zhou, D. Highly Sensitive Electronic Skin with a Linear Response Based on the Strategy of Controlling the Contact Area. *Nano Energy* **2021**, *85*, 106013.
(50) Sivan, V.; Tang, S.-Y.; O'Mullane, A. P.; Petersen, P.; Eshtiaghi, N.; Kalantar-zadeh, K.; Mitchell, A. Liquid Metal Marbles. *Adv. Funct. Mater.* **2013**, *23*, 144.
(51) Doudrick, K.; Liu, S.; Mutunga, E. M.; Klein, K. L.; Damle, V.; Varanasi, K. K.; Rykaczewski, K. Different Shades of Oxide: From Nanoscale Wetting Mechanisms to Contact Printing of Gallium-Based Liquid Metals. *Langmuir* **2014**, *30*, 6867.
(52) Kramer, R. K.; Boley, J. W.; Stone, H. A.; Weaver, J. C.; Wood, R. J. Effect of Microtextured Surface Topography on the Wetting Behavior of Eutectic Gallium−Indium Alloys. *Langmuir* **2014**, *30*, 533.
(53) Zhang, C.; Yang, Q.; Shan, C.; Zhang, J.; Yong, J.; Fang, Y.; Hou, X.; Chen, F. Tuning a Surface Super-Repellent to Liquid Metal by a Femtosecond Laser. *RSC Adv.* **2020**, *10*, 3301.
(54) Zhang, J.; Zhang, K.; Yong, J.; Yang, Q.; He, Y.; Zhang, C.; Hou, X.; Chen, F. Femtosecond Laser Preparing Patternable Liquid-Metal-Repellent Surface for Flexible Electronics. *J. Colloid Interface Sci.* **2020**, *578*, 146.
(55) Zhang, C.; Yang, Q.; Yong, J.; Shan, C.; Zhang, J.; Hou, X.; Chen, F. Guiding Magnetic Liquid Metal for Flexible Circuit. *Int. J. Extrem. Manuf.* **2021**, *3*, 025102.
(56) Yong, J.; Zhang, C.; Bai, X.; Zhang, J.; Yang, Q.; Hou, X.; Chen, F. Designing "Supermetalphobic" Surfaces that Greatly Repel Liquid Metal by Femtosecond Laser Processing: Does the Surface Chemistry or Microstructure Play a Crucial Role? *Adv. Mater. Interfaces* **2020**, *7*, 1901931.
(57) Li, H.; Zhu, G.; Shen, Y.; Han, Z.; Zhang, J.; Li, J. Robust Superhydrophobic Attapulgite Meshes for Effective Separation of Water-in-Oil Emulsions. *J. Colloid Interface Sci.* **2019**, *557*, 84.

(58) Li, H.; Mu, P.; Li, J.; Wang, Q. Inverse Desert Beetle-Like ZIF-8/PAN Composite Nanofibrous Membrane for Highly Efficient Separation of Oil-in-Water Emulsions. *J. Mater. Chem. A* **2021**, *9*, 4167.
(59) Yong, J.; Chen, F.; Fang, Y.; Huo, J.; Yang, Q.; Zhang, J.; Bian, H.; Hou, X. Bioinspired Design of Underwater Superaerophobic and Superaerophilic Surfaces by Femtosecond Laser Ablation for Anti- or Capturing Bubbles. *ACS Appl. Mater. Interfaces* **2017**, *9*, 39863.
(60) Genzer, J.; Efimenko, K. Creating Long-Lived Superhydrophobic Polymer Surfaces Through Mechanically Assembled Monolayers. *Science* **2000**, *290*, 2130.
(61) Jia, Y.; Wang, S.; Chen, F. Femtosecond Laser Direct Writing of Flexibly Configured Waveguide Geometries in Optical Crystals: Fabrication and Application. *Opto-Electron. Adv.* **2020**, *3*, 190042.
(62) Livakas, N.; Skoulas, E.; Stratakis, E. Omnidirectional Iridescence via Cylindricallypolarized Femtosecond Laser Processing. *Opto-Electron. Adv.* **2020**, *3*, 190035.
(63) Wan, Z.; Chen, X.; Gu, M. Laser Scribed Graphene for Supercapacitors. *Opto-Electron. Adv.* **2021**, *4*, 200079.
(64) Zhang, D.; Sugioka, K. Hierarchical Microstructures with High Spatial Frequency Laser Induced Periodic Surface Structures Possessing Different Orientations Created by Femtosecond Laser Ablation of Silicon in Liquids. *Opto-Electron. Adv.* **2019**, *2*, 19000201.
(65) Yong, J.; Yang, Q.; Huo, J.; Hou, X.; Chen, F. Underwater Gas Self-Transportation Along Femtosecond Laser-Written Open Superhydrophobic Surface Microchannels (<100 μm) for Bubble/Gas Manipulation. *Int. J. Extrem. Manuf.* **2022**, *4*, 015002.

https://doi.org/10.1021/acsami.2c08835
ACS Appl. Mater. Interfaces 2022, 14, 38328−38338